Salemme, F. R. (1978) *Annu. Rev. Biochem. 46*, 299–329.
Scholes, C. P., & Malmstrom, B. G. (1986) *FEBS Lett. 198*, 125–129.
Shire, S. J., Hanania, G. I. H., & Gurd, F. R. N. (1974) *Biochemistry 13*, 2967–2974.
Simondsen, R. P., & Tollin, G. (1983) *Biochemistry 22*, 3008–3016.
Simondsen, R. P., Weber, P. C., Salemme, F. R., & Tollin, G. (1982) *Biochemistry 21*, 6366–6375.
Smith, W. W., Burnett, R. M., Darling, G. D., & Ludwig, M. L. (1977) *J. Mol. Biol. 117*, 195–225.
Tanford, C., & Roxby, R. (1972) *Biochemistry 11*, 2192–2195.
Tollin, G., Cheddar, G., Watkins, J. A., Meyer, T. E., & Cusanovich, M. A. (1984) *Biochemistry 23*, 6345–6349.
Tollin, G., Hanson, L. K., Caffrey, M., Meyer, T. E., & Cusanovich, M. A. (1986) *Proc. Natl. Acad. Sci. U.S.A. 83*, 3693–3697.
Waldmeyer, B., & Bosshard, H. R. (1985) *J. Biol. Chem. 260*, 5184–5190.
Waldmeyer, B., Bechtold, R., Bosshard, H. R., & Poulos, T. L. (1982) *J. Biol. Chem. 257*, 6073–6076.
Wittenberg, B., Kampa, L., Wittenberg, J. B., Blumberg, W. E., & Peisach, J. (1968) *J. Biol. Chem. 243*, 1863–1870.
Yonetani, T. (1967) *Methods Enzymol. 1*, 336–339.
Yonetani, T. (1976) *Enzymes (3rd Ed.) 18C*, 345–361.

# Conductance Routes for Protons across Membrane Barriers†

John Bramhall
*Department of Microbiology and Immunology and The Jonsson Comprehensive Cancer Center, School of Medicine, University of California, Los Angeles, California 90024*

*Received June 30, 1986; Revised Manuscript Received November 18, 1986*

ABSTRACT: Simple phospholipid bilayers show a high level of permeability to protons; in spite of this fact, large proton gradients existing across such bilayers may decay very slowly. In sealed systems, the free movement of protons across a membrane barrier is severely restricted by the coincident development of a proton diffusion potential. Using the fluorescent weak acid *N*-[5-(dimethylamino)naphth-1-ylsulfonyl]glycine (dansylglycine) to monitor the collapse of pH gradients across barrier membranes, it is revealed that in strongly buffered systems movement of the small number of protons giving rise to this electrical potential is insufficient to perturb the proton concentration gradient; significant flux of protons (and hence significant collapse of the concentration gradient) can only occur (a) if protons traverse the membrane as part of an electroneutral complex or (b) if there is a balancing flow of appropriate counterions. In both instances, proton flux is obligatorily coupled to the translocation of species other than protons. In weakly buffered systems, the small initial uncoupled electrogenic flux of protons may significantly alter the concentration gradient. This initial rapid gradient collapse caused by uncoupled electrogenic proton movements is then superimposed upon the residual collapse attributable to tightly coupled proton flux. The initial uncoupled electrogenic proton flux shows a temperature dependence very similar to that demonstrated for water permeation across simple lipid bilayers; upon cooling, there is a sharp decrease in flux at the temperature coinciding with the main gel–liquid-crystalline phase transition of the lipid. The coupled proton flux shows a markedly different temperature dependence with no dramatic change in rate at the phase transition temperature and strong similarity to the behavior previously seen with solutes known to be permeating as electrically neutral compounds. This temperature dependence profile for proton permeation supports the suggestion that this process has much more in common with water diffusion than with the translocation of other monovalent cations, such as $Na^+$, across membrane barriers.

The electrochemical proton gradient $\Delta\tilde{\mu}_{H^+}$, existing across the inner membrane of the mitochondrion and the cytoplasmic membrane of most bacterial cells, is believed to be the primary intermediate linking respiration to active ion transport and then to synthesis of ATP (Mitchell, 1979). Although $\Delta\tilde{\mu}_{H^+}$ is generally not accompanied by large chemical proton gradients, there are several examples, most notably that of the chloroplast thylakoid membrane, but also including the endosomal and lysosomal boundary membranes of most eukaryotic cells, of relatively substantial proton concentration gradients ($\Delta$pH) being maintained across biological membranes (Hinkle & McCarty, 1978; Helenius et al., 1985). These large chemical gradients are generally estabished by the action of integral membrane proton pumps (Forgac et al., 1983) and are assumed to be stabilized by the combined effects of an intrinsically low proton permeability of the boundary membrane and the low concentration (<10 $\mu$M) of protons in the surrounding environment. The vital significance of $\Delta\tilde{\mu}_{H^+}$ and $\Delta$pH to cellular metabolism, coupled with the fact that the principal obstacles to free permeation of polar solutes and ions across the endosomal, thylakoid, and mitochondrial matrix boundary membranes are created primarily by the impenetrable nature of the lipid matrix (Deamer & Bramhall, 1986), has prompted several attempts to quantify the proton permeability of lipid bilayers of defined composition. These measurements have established that protons permeate lipid bilayers several orders of magnitude faster than other small cations such as sodium or potassium and that, in fact, most membranes show a rel-

† Supported by grants from the Cancer Research Coordinating Committee of the University of California and from the UCLA Academic Senate.

0006-2960/87/0426-2848$01.50/0 

atively high level of permeability for $H^+/OH^-$. The best estimates for the true proton/hydroxide permeability coefficients of these model membranes fall within the range $10^{-7}$–$10^{-4}$ cm·s$^{-1}$ (Nichols & Deamer, 1980; Cafiso & Hubbell, 1983). Although a precise mechanical explanation for this high permeability to protons is still lacking, one possibility is that rapid $H^+/OH^-$ translocation requires the presence of transient projections of water into the hydrophobic domain of the bilayer (Nichols & Deamer, 1980), such structures being capable of providing a conduit for protons directly into the hydrophobic domain, a suggestion strongly supported by the studies of Elamrani and Blume (1983) and Lawaczeck et al. (Pitterich & Lawaczeck, 1985; Engelbert & Lawaczeck, 1985) which certainly focus attention on similarities between proton and water permeation rates. Note that, although it may be presumed to be perfectly possible for water intercalated into the membrane to form continuous strands traversing the entire thickness of the bilayer, there is no necessity for the projections to span the membrane in order to catalyze proton permeation. If, indeed, proton flux is catalyzed by membrane water, then proton conductance measurements are likely to yield much useful information about this aspect of intrabilayer water structure.

The paradox apparent in the maintenance of substantial chemical proton gradients across membranes whose intrinsic $H^+/OH^-$ permeability is quite high is largely explained by the direct observation that free permeation of either protons or hydroxide ions is electrogenic and must thus become entrained to the movement of appropriate counterions (Deamer & Nichols, 1983). Indeed, studies of model systems consisting of pure phospholipid bilayers have demonstrated not only that collapse of $\Delta$pH can lead to the generation of $\Delta E_m$, a transmembrane electrical potential (Cafiso & Hubbell, 1983), but also that $\Delta$pH can develop upon the establishment of $\Delta E_m$ (Krishnamoorthy & Hinkle, 1984; Garcia et al., 1984). Although it is difficult to discriminate, experimentally, between fluxes of $H^+/H_3O^+$ ions and equal but opposite fluxes of $OH^-$ ions, particularly when the measured parameter is $\Delta$pH, it is operationally convenient to define changes in $\Delta$pH as the result of net movement of free protons (i.e., flux of a small cation). In general, the permeability of saturated phospholipid bilayers to small cations is extremely low (Papahadjopoulos et al., 1973; Parsegian, 1969), much lower than to protons themselves [for a review, see Deamer and Bramhall (1986)]. One might expect that under these circumstances the permeation of protons should be constrained by electrostatic forces generated by the proton diffusion potential (Bramhall, 1984) and that pH gradients existing across lecithin bilayers would collapse relatively slowly when the only counterions present are unable to cross the membrane barrier. However, the existence of an alternative, nonelectrogenic route of proton permeation as part of a neutral acid molecule would account for the rapid collapse of pH gradients that has been observed with simple lipid systems in the presence of inorganic anions such as $Cl^-$ and $NO_3^-$ (Gutknecht & Walter, 1981; Nozaki & Tanford, 1981). In this report, I describe an experimental system that permits ready distinction between uncoupled electrogenic proton permeation (possibly attributable to conductance along water strands), coupled proton permeation regulated by movements of small counterions such as $Na^+$, and the electroneutral proton flux catalyzed by the free diffusion of discharged inorganic acids across the barrier membrane.

## Materials and Methods

*Preparation of Lipid Bilayers.* The purity of phospholipids [dimyristoylphosphatidylcholine (DMPC),[1] DPPC, and DSPC] supplied by Sigma (St. Louis, MO) was verified by TLC on silica gel using a developing solvent of chloroform/methanol/glacial acetic acid/water (90:40:12:2 v/v). Small unilamellar lipid vesicles were prepared by sonication of lipid suspensions in aqueous buffer under an atmosphere of nitrogen. Lipid was dissolved in chloroform/methanol (2:1 v/v), aliquoted into glass tubes, dried under nitrogen at 40 °C, and placed under high vacuum for 18–20 h at 20 °C to remove residual chloroform before use. Typically, 50 mg of DPPC was sonicated in 1 mL of buffer (5 mM sodium phosphate, pH 8.0, containing 50 mM sodium sulfate). Sonication was performed by using a microprobe for 15 min at a power setting of 30–35 W; the temperature of the lipid suspension was maintained at 5 °C above the lipid's melting point ($T_c$ + 5 °C, i.e., at 46 °C for DPPC) throughout the sonication process. The vesicle preparation was centrifuged (100000$g$, 30 min) to remove structures other than small vesicles and then stored at $T_c$ + 5 °C prior to use; fresh vesicles were made daily.

*Molecular Sieve Chromatography.* In the case of vesicles containing trapped $^{22}$NaCl or $K^{51}CrO_4$, the vesicle preparation was cooled to at least 20 °C below the lipid melting point ($T_c$ − 20 °C) and then separated from untrapped isotope by preparative gel permeation chromatography using a Bio-Rad P-10 gel (0.5 × 17 cm column) equilibrated with isotonic buffer (generally 50 mM sodium phosphate adjusted to pH 7.4). The vesicles eluted with the void volume and were used immediately. Analytical gel permeation chromatography was performed by using Sepharose CL-2B (0.5 × 43 cm column) under essentially similar conditions. Aqueous captured volume:lipid ratios were calculated from the trapped:free $^{22}$Na or $^{51}$Cr ratio; the relative lipid content of vesicle preparations was determined by fluorescence assay using diphenylhexatriene (London & Feigenson, 1978).

*Measurement of Sodium Permeation across the Vesicle Boundary Membrane.* Equilibrium measurements of $^{22}$Na leakage from DPPC vesicles were performed by using plastic multiwell microdialysis chambers with a 200-$\mu$L cavity on each side of a semipermeable membrane ($M_r$ 12000 cutoff), as previously described (Bramhall, 1984). A suspension of vesicles, containing entrapped $^{22}$NaCl, was placed in one compartment and an equal volume of isotonic buffer placed in the other. The microdialysis cells were rotated at approximately 15 rpm for 8 h at the experimental temperature. Proportional release of $^{22}$Na from vesicles was determined from the ratio of the radioactivity of the vesicle-free compartment ($Q_a$) to the total radioactivity of the two compartments ($Q_t$) according to eq 1.

$$\text{proportional release} = 2Q_a/Q_t \quad (1)$$

*Determination of Proton Concentration Gradients.* Dansylglycine was obtained from Sigma Chemical Co. and was purified before use by thin-layer chromatography on silica gel using a developing solvent of chloroform/methanol (2:1 v/v). Purified material ($R_f$ 0.24) was eluted from the adsorbent by using methanol and stored as a $10^{-2}$ M solution in absolute ethanol at −20 °C. The use of this fluorescent dye to monitor the magnitude and stability of transmembrane pH gradients has been fully described in a previous report (Bramhall, 1986a). Briefly, a suspension of phospholipid vesicles, containing an internal trapped buffer with $pH_i$, is diluted, at time zero, into isoosmotic buffer with $pH_o$ at a defined experimental

[1] Abbreviations: DMPC, dimyristoylphosphatidylcholine; DPPC, dipalmitoylphosphatidylcholine; DSPC, distearoylphosphatidylcholine; dansyl, 5-(dimethylamino)naphthalene-1-sulfonyl; $T_c$, lipid gel–liquid-crystalline phase transition temperature; TLC, thin-layer chromatography.

temperature. For most of the experiments described in this report, 50 μL of a 50 mg/mL lipid suspension in 50 mM sodium sulfate buffered to pH 8.0 with 5 mM sodium phosphate was transferred to a cuvette containing 2 mL of 50 mM sodium sulfate and 0.5 μM dansylglycine buffered to pH 6.0 with 5 mM sodium phosphate. This established a ΔpH of 2 units at zero time and gave a final phospholipid concentration of 1.66 mM. Fluorescence intensity of the sample was monitored continuously (at 510 nm) until the complete collapse of ΔpH was triggered by the addition of 10 μL of 5 M sodium acetate adjusted to pH 6.0 with acetic acid. In certain experiments, extremely slow rates of ΔpH collapse were measured by recording the sample fluorescence emission intensity discontinuously at time intervals after the establishment of a proton concentration gradient. Vesicle suspensions were maintained in borosilicate glass tubes, subjected to continuous gentle stirring, and maintained at the experimental temperature by immersion in a precisely regulated circulating water bath located in a cold room operating at 8 °C. At appropriate time intervals, 2-mL aliquots from the samples were transferred to a quartz cuvette, previously equilibrated to the same experimental temperature, for fluorescence assay. Fluorescence and light-scattering measurements were performed with a Fluorolog II spectrometer (Spex Industries, Metuchen, NJ) equipped with temperature control accessories and a magnetic stirrer and using an exciting radiation of 350 nm. Sample temperatures were monitored with a platinum resistance thermometer housed in the optical cuvette.

## Results and Discussion

In this study, I sought to differentiate between uncoupled electrogenic movements of protons (i.e., net flux of $H^+/OH^-$ across a membrane barrier in the absence of counterion movement), electrogenic proton flux tightly coupled to counterion permeation, and electrically silent proton flux catalyzed by the permeation of discharged acids. Each of these processes is likely to show a different, characteristic rate dependence on temperature. For example, the permeability of saturated lecithin bilayers to sodium ions shows a sharp maximum at $T_c$, the temperature of the main gel to liquid-crystalline phase transition (Papahadjopoulos et al., 1973; El-Mashak & Tsong, 1985). If proton flux is coupled to, and limited by, counterflow of sodium ions across the membrane barrier, then we would predict that the proton flux would also show a rate maximum at $T_c$. I reasoned that measurements of the relative rates of ΔpH collapse over a range of experimental temperatures should provide useful information about the rate-limiting factors for proton permeation.

The use of dansylglycine provides an excellent method for making such measurements. The dye is a fluorescent weak acid that binds to, and permeates across, many types of lipid bilayers (Bramhall, 1985). In general, binding and permeation occur with substantially different rates (translocation across the bilayer being orders of magnitude slower than the initial binding event), but both processes are reflected in substantial changes in fluorescence properties. The initial binding event elicits a sharp increase in the fluorescence intensity for the system as the dansyl chromophore, which is extremely sensitive to changes in the dieletric constant of its surrounding environment, becomes embedded in the hydrocarbon phase of the outer membrane monolayer. There is a second, slower, phase of fluorescence intensity increase associated with population of the inner monolayer with dye. Because the dye permeates lipid bilayers as a neutral species (Bramhall, 1984, 1986a), the flux of dye across the membrane is strongly dependent on the degree of protonation of the dye's carboxylate moiety, and hence on the environmental pH. When the external pH is lower than that of the internal compartment, the inward flux of dye is greater than that in the opposite direction, and the dye accumulates in the vesicle lumen. This leads to a local elevation of the dansylglycine concentration in the inner membrane monolayer, which in turn results in an elevated fluorescence intensity proportional to the membrane pH gradient. I have previously demonstrated how fluorescence measurements can be used to monitor the kinetics of dye translocation (Bramhall, 1984) and how these kinetics can be related to the existence of transmembrane proton concentration gradients (Bramhall, 1986a). For the experiments reported here

$$\Delta pH = k \log \Delta F_m \quad (2)$$

where $\Delta F_m$ is the difference between sample fluorescence intensities measured in the absence and presence of a pH gradient and $k$ is an empirical proportionality constant. Thus, fluorescence intensity is directly proportional to the proton concentration gradient existing across the membrane barrier.

*Spontaneous Collapse of ΔpH.* In view of the fact that, under the experimental conditions reported here, dansylglycine fluorescence intensity was directly proportional to pH it was to be expected that a slowly declining proton concentration gradient would give rise to a slowly declining fluorescence signal intensity. Figure 1 shows that when DSPC vesicles, containing 100 mM sodium phosphate, pH 8.0, were suspended in isoosmotic (137 mM) sodium phosphate, pH 6.0, there was an initial sharp increase in sample fluorescence intensity, followed by a slow decline which accelerated immediately upon the addition of sodium acetate, a salt known to collapse pH gradients under these experimental conditions (Bangham et al., 1967).[2] Both the increase and decline phases showed a clear rate dependence on temperature. The initial fluorescence intensity increase (which occurs as dansylglycine binds to, and equilibrates across, the boundary membrane) has been extensively investigated and described previously (Bramhall, 1984, 1985, 1986a; Jähnig & Bramhall, 1982); the temperature dependence of the subsequent slow decline in fluorescence intensity in the presence in ΔpH is the subject of this report.

The decline in fluorescence intensity resulted from a reequilibration of dansylglycine in response to the changing ratio of $[H^+]$ across the membrane. Under the conditions described in Figure 1, the decline was usually a simple monoexponential process (Figure 1B) characterized by a single rate constant, $k''$. When the pH gradient collapsed at a rate which was slow with respect to the time constant for dansylglycine equilibration (e.g., in the absence of acetate), then the initial rate of decrease in fluorescence intensity corresponded to the initial rate of collapse of ΔpH:

$$dF/dt = -d[H^+]_i/dt \quad (3)$$

$$\ln [F_0/F_t] = k''t \quad (4)$$

where $[H^+]_i$ is the free proton concentration of the internal aqueous compartment and $F_0$ and $F_t$ are the initial fluorescence intensity and the intensity at time $t$, respectively. Note that because the external pH was constant, the rate of change of fluorescence simply reflected the rate of change in pH of the internal compartment caused by the net flux of protons into the vesicle lumen.[3]

[2] When ammonium acetate is present, ΔpH collapses too rapidly for any kinetic analysis (the rate of collapse is greater than the rate of equilibration of dye concentrations across the bilayer). In the absence of sodium acetate, the fluorescence intensity declines, at a constant rate, to the same final value; acetate merely accelerates the attainment of final equilibrium.

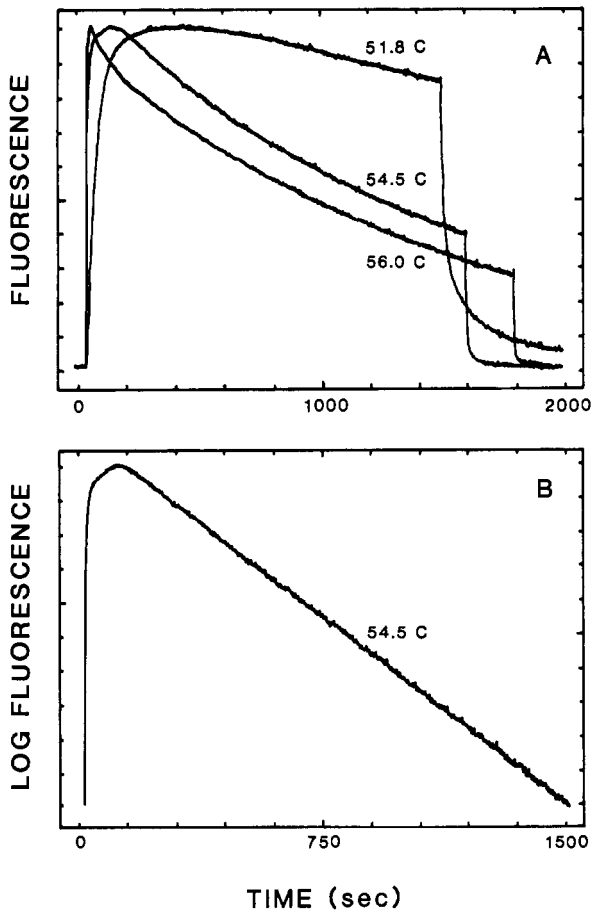


FIGURE 1: Dansylglycine reports the rate of collapse of proton gradients. (A) Small, unilamellar DSPC vesicles containing 100 mM sodium phosphate, pH 8.0, were diluted 1:40 into 137 mM sodium phosphate, pH 6.0, containing $5 \times 10^{-7}$ M dansylglycine. The diluting buffer was held in a quartz cuvette inside the temperature-controlled sample cavity of the fluorescence spectrometer. Fluorescence emission intensity (510 nm) was recorded continuously during the vesicle addition and during the subsequent addition of sodium acetate to a final concentration of 25 mM. Final lipid concentration of the sample was 1.3 mM; experimental temperatures were 51.8, 54.5, and 56.0 °C. (B) Data obtained from mixing experiment performed at 54 °C and plotted according to a first-order rate equation.

*Effect of Buffer Strength.* Although it has been clearly demonstrated that lecithin bilayers show very high intrinsic permeability to protons (Nichols & Deamer, 1980; Cafiso & Hubbell, 1983), in sealed systems it is possible for the free movement of protons across a membrane to become severely restricted by development of $\Delta E_m$ created by the flow of

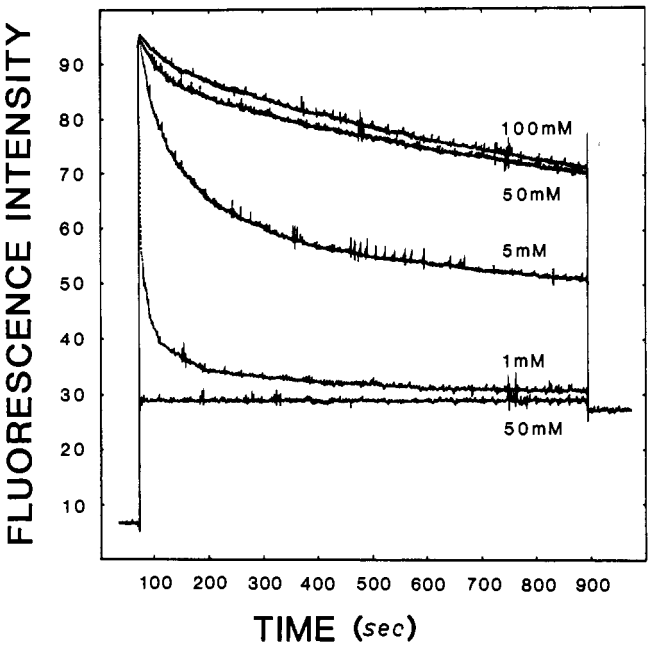


FIGURE 2: Effect of buffer capacity on collapse of ΔpH. Small, unilamellar DPPC vesicles containing sodium phosphate buffer, pH 8.0, were diluted (1:40) into sodium phosphate buffer maintained at 42 °C in the sample cavity of the fluorescence spectrometer. The lowermost trace was obtained when vesicles containing 50 mM sodium phosphate, pH 8.0, were diluted into identical buffer. The upper four traces were obtained when vesicles containing (from the top) 100 mM sodium phosphate, 50 mM sodium phosphate, 5 mM sodium phosphate/50 mM sodium sulfate, or 1 mM sodium phosphate/50 mM sodium sulfate (all buffered to pH 8.0) were diluted into corresponding buffers adjusted to pH 6.0. In each case, the diluting buffer also contained dansylglycine ($5 \times 10^{-7}$ M). The fluorescence intensity of each sample was monitored continuously during and after addition of the vesicles and the subsequent addition of sodium acetate, to a final concentration of 25 mM.

positive charge across the barrier. According to Mitchell and Moyle (1968), $\Delta\tilde{\mu}_{H^+}$ is defined by eq 5.

$$\Delta\tilde{\mu}_{H^+} = \Delta E_m - (2.3RT/F)\Delta pH \quad (5)$$

When $\Delta E_m$ exactly balances the energy of ΔpH, $\Delta\tilde{\mu}_{H^+}$ (the force driving net flux of protons across the membrane) becomes equal to zero, and net proton flux stops. Under the conditions described in Figure 1, the small number of protons that must traverse the bilayer in order to develop $\Delta E_m$ exactly balancing the energy of the chemical potential of the applied pH gradient was insufficient to perturb the gradient itself; the strong buffer capacity of the vesicle lumen effectively resisted changes in internal pH. This means, a priori, that the collapse of ΔpH actually observed could not be occurring by electrogenic movement of protons alone; the process must have involved either copermeation of appropriate counterions or translocation of protons as part of an electroneutral complex (e.g., discharged acid).[4]

[3] Rates of change of fluorescence intensity can only reflect the kinetics of pH gradient collapse when the permeation rate of the reporter molecule (dansylglycine) is non rate limiting. Extensive and precise measurements of the rates of translocation of this dye across lipid bilayers of different defined composition have been carried out under a very wide variety of experimental conditions (Bramhall, 1986a,b). Under all the conditions described in this paper, the rate of translocation of dansylglycine across the appropriate boundary membrane was never less than 1 order of magnitude faster than the corresponding rate of collapse of the pH gradient; indeed, it was on most occasions several orders faster. The only exception to this generality was when the pH gradients were suddenly collapsed by the addition of sodium acetate. In the presence of acetate, dye translocation is much slower than the rate of collapse of the proton concentration gradient (because of the rapid permeation of acetic acid into the lumen of the vesicle), and fluorescence intensity changes no longer reflect the rate of change of the pH gradient. The sudden decreases in fluorescence intensity that accompany acetate addition confirm that dye translocation kinetics are not rate limiting in the earlier stages of each experiment (where fluorescence intensity changes are characteristically very much slower).

[4] Direct determination of trapped volume and phospholipid content of the vesicle preparations used in the experiment depicted in Figure 1 reveals that the fluorescence cuvette contained sufficient phospholipid (2.5 mg) to generate 7000 $cm^2$ of membrane [assuming a projected area of 0.7 $nm^2$ per phospholipid molecule (Small, 1967; Lis et al., 1982; Cornell & Separovic, 1983)] defining an entrapped volume of $1.5 \times 10^{-3}$ $cm^3$ (measured capture volume was 0.5 L/mol of DSPC). The internal and external buffers are 100 and 137 mM sodium phosphate, pH 8.0 and 6.0, respectively; thus, complete collapse of ΔpH entails movement of $7.41 \times 10^{16}$ protons from the external to the internal compartment. This corresponds to movement of 18.3 $C/cm^2$ if the entire membrane surface area of the sample is involved in this translocation, which, in turn, implies development of an impossibly large membrane potential ($\Delta E_m$ = 1.8 V assuming a membrane capacitance of 1 $\mu F/cm^2$).

Although strong internal buffer resists the effects of migrating protons, it could be predicted that, were the buffer capacity of the lumen to be substantially decreased, the small initial uncoupled flux of protons into the vesicle might be sufficient to effect a significant decrease in internal pH before becoming arrested by $\Delta E_m$. The use of phospholipid bilayers in the form vesicles greatly facilitates detection of this initial phase of ΔpH collapse. Sonication of lipid dispersions greatly increases the membrane surface area:trapped volume ratio,[5] and the relatively small internal (trapped) volume of such preparations enhances, sharply, the changes in lumenal proton concentration caused by any given flux of protons across the boundary bilayer. This combination of low buffer capacity within small vesicles was expected to optimize the responses of dansylglycine to initial, uncoupled proton flux. Figure 2 shows that the effect of reducing internal buffer strength was to promote a fast initial collapse of ΔpH that became increasingly pronounced with progressively smaller internal buffer capacity and gave rise to a biphasic form to the overall decrease in fluorescence intensity.

This biphasic decline in ΔpH could have resulted either from the behavior of two discrete populations of vesicles or, alternatively, from two phases of decrease in the pH of the entrapped buffer within each vesicle. Because (a) all vesicles were manufactured from the same batch of DPPC using a standard procedure, (b) each preparation showed similar trapping efficiency and capture volume (0.5 L/mol of phospholipid), (c) the appearance of the rapid phase of fluorescence decrease correlated with decreasing buffer capacity of the entrapped solution and not with its ionic strength, and (d) the rapid phase could be eliminated by dialyzing vesicles containing weak buffer against stronger buffer prior to generation of ΔpH (data not shown), I have interpreted the rapid phase of fluorescence as being the consequence of rapid change (decrease) in the internal pH of a homogeneous population of small vesicles, a change that is only apparent in the presence of weak buffer, even with small vesicles, and which thus probably involves transit of a limited number of protons across the boundary membrane.

Thus, when ΔpH was imposed in the presence of 5 mM sodium phosphate buffer, its subsequent collapse occurred in two discrete phases. There was an initial phase, attributable to free permeation of $H^+$ across the barrier membrane into the vesicle lumen; this must involve charge separation across the bilayer and must become arrested by the coincident development of $\Delta E_m$ and hence become unable to lead to complete collapse of ΔpH under most experimental circumstances. This event was followed by a second phase of proton movement which must be tightly coupled to, and therefore rate limited by, the concatenant movement of appropriate counterions across the membrane barrier, leading ultimately to total collapse of ΔpH. In the systems under consideration, the only possible counterions are $Na^+$ (which would have to exit the vesicle lumen as protons enter) and phosphate anion (which would migrate in the same direction as protons).

*Temperature Dependence of Coupled Proton Flux.* Figure 1 showed that the slow, coupled phase of $H^+$ flux (the only phase observed in the presence of high buffer capacity) exhibits a rate dependence on temperature. If proton permeation does indeed become entrained to copermeation of, for example, $Na^+$ counterions, then we might expect the rate of collapse of ΔpH to show the same temperature dependence profile as sodium permeation rates. Table I demonstrates that the vesicles used in these studies displayed a maximum rate of sodium leakage in the region of $T_c$, the temperature of the major gel–liquid-crystalline phase transition, confirming the original observations of Papahadjopoulos et al. (1973) and El-Mashak and Tsong (1985). This behavior was not influenced to any appreciable extent by the presence of dansylglycine even at a dye:lipid molar ratio 7-fold higher than that used experimentally.

Figure 3 illustrates the Arrhenius plot of temperature vs. rate of collapse of ΔpH for DMPC bilayers monitored in the presence of strong (50 mM phosphate) buffer. The plot ex-

[5] To give some feeling for the quantities involved, for the generation of data described in Figure 2, the optical cuvette contained approximately 5000 $cm^2$ of membrane (2 mg of DPPC) enclosing a trapped volume of 1.3 μL.

Table I: Effect of Dansylglycine on Membrane Integrity[a]

| dye:lipid ratio | leakage of $^{22}Na$ (% ± SD) at 4 °C | 22 °C | 41 °C | 48 °C |
|---|---|---|---|---|
| 1:500 | 7.4 ± 0.9 | 9.8 ± 0.8 | 94.6 ± 1.9 | 65.8 ± 1.9 |
| control | 6.4 ± 0.3 | 9.1 ± 0.1 | 93.1 ± 5.1 | 67.2 ± 3.1 |

[a] Leakage of $^{22}Na$ from DPPC vesicles was measured by equilibrium dialysis, as described under Materials and Methods. Spontaneous sodium leakage was measured in the presence or absence of dansylglycine. The concentration of dansylglycine tested, 10 μM, corresponds to a dye:lipid molar ratio of 1:500 (7× higher than those encountered during actual use of the probe). Measurements of leakage were made after incubation at one of four experimental temperatures for 8 h. Release of $^{22}Na$ is expressed as a percentage of the total $^{22}Na$ originally trapped within the sample vesicle.

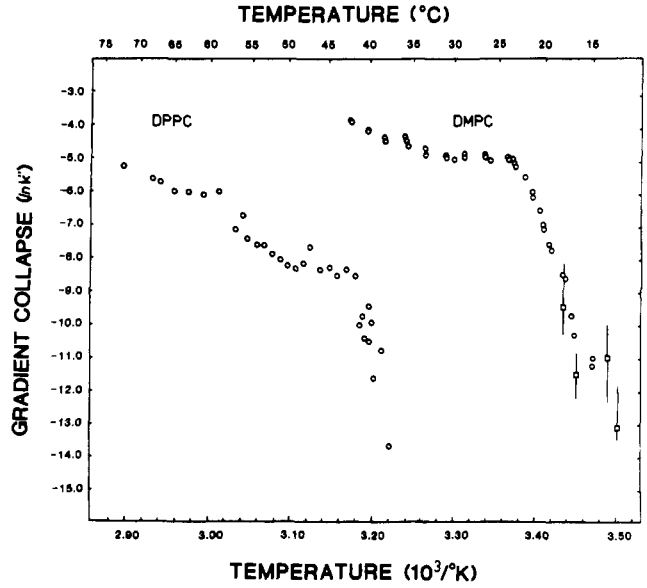


FIGURE 3: Temperature dependence of coupled proton flux across phospholipid bilayers. (DMPC) Fifty microliters of a suspension of small DMPC vesicles in 50 mM sodium phosphate, pH 8.0 (lipid concentration 50 mg/mL), was diluted into 2 mL of 68 mM sodium phosphate, pH 6.0, containing $5 \times 10^{-7}$ M dansylglycine. (DPPC) Fifty microliters of a suspension of small DPPC vesicles in 50 mM sodium sulfate buffered to pH 8.0 with 5 mM sodium phosphate was diluted into 2 mL of 50 mM sodium sulfate buffered to pH 6.0 with 5 mM sodium phosphate and containing $5 \times 10^{-7}$ M dansylglycine; final lipid concentration was 2.5 mg/mL. For both DMPC and DPPC, the diluting buffer was held in the quartz sample compartment of the fluorescence spectrometer and was maintained at a defined experimental temperature. The fluorescence emission intensity (510 nm) was recorded continuously, and the initial rate of decreased in fluorescence ($k'$) was calculated from a first-order rate equation by inserting, as a terminal value, the fluorescence intensity obtained after the addition of 20 μL of 1 M sodium acetate to the sample cuvette. $k'$ was determined at several experimental temperatures and is plotted here in the form of an Arrhenius function. The points marked (□) represent the mean and *range* of five discontinuous rate measurements made at each of four experimental temperatures, as described under Materials and Methods.

tends from 20 °C above $T_c$ to 12 °C below and shows only one major change in slope, coinciding with the melting point of the bilayer. Figure 3 also shows the Arrhenius plot for the second, slow (coupled) ΔpH collapse across DPPC bilayers monitored in the presence of weak (5 mM phosphate) buffer. In this case, the plot extends from 30 °C above $T_c$ to 5 °C below and also shows only one major change in slope, again coinciding with the bilayer main phase transition. The exceptionally slow rates for ΔpH collapse at temperatures more than 5 °C below $T_c$ ($t_{1/2}$ = 2 months at 35 °C with DPPC) made accurate rate determinations difficult to collect at lower temperatures and thus limited the available temperature range for the DPPC plot. Even using DMPC, which shows an intrinsically higher permeability to the solutes responsible for collapse of the pH gradient, it was only possible to make meaningful measurements of ΔpH collapse rates below 15 °C by resorting to use of discontinuous readings of sample fluorescence intensity over extended intervals of time. These data show considerable scatter caused, primarily, by the very small changes in signal amplitude associated with very slow rates of gradient collapse. Despite these technical difficulties, the overall similarities between the sets of data obtained with the two homologous phospholipids made it reasonable to conclude that the coupled phase of ΔpH collapse (monitored in the presence of either weak or strong buffer capacity) showed no similarity at all to the permeation behavior of $Na^+$ but instead displayed an overall pattern identical with that observed previously for solutes permeating as electrically neutral species (Bramhall, 1984, 1986a).

It seems safe to conclude, then, that the collapse of ΔpH was not in fact rate limited by $Na^+$ permeation and that the proton flux responsible for collapse of ΔpH was not, therefore, entrained to sodium flux. The only alternative counterion in the experimental system used was phosphate. At pH 6.0 (the external pH), approximately 86% of the available phosphate was in the form of the monobasic anion $H_2PO_4^-$, which could migrate to the vesicle lumen in 1:1 stoichiometry with $H^+$. It is worth noting, however, that the external phosphate buffer also contained a small but possibly highly significant number of undissociated $H_3PO_4$ molecules (approximately 1:7000 total phosphate). Diffusion of this $H_3PO_4$ across the boundary membrane, followed by dissociation in the internal space, would provide a highly efficient mechanism for proton translocation, one which, furthermore, avoids the necessity for any charged species to penetrate the lipid bilayer. Figure 4 illustrates the consequences of varying proton and phosphate concentration ratios at each face of the vesicle boundary membrane. It was not possible in these experiments to establish a substantial proton concentration gradient while maintaining no gradient of $H_3PO_4$ across vesicle boundary membranes. When, however, $H_2PO_4^-$ concentrations on each side of the membrane were equal, there was still significant collapse of ΔpH under circumstances where the $H_3PO_4$ concentration of the vesicle lumen was sustantially lower than that of the external medium (Figure 4A). Conversely, when the internal phosphate concentration was made substantially higher than that of the external medium, ΔpH was generated, presumably by the net efflux of protonated phosphate from the vesicle lumen, resulting in a steady increase in dansylglycine fluorescence intensity (Figure 4C). Although the present experiments fail to provide an absolute distinction between coupled flux of $H_2PO_4^-/H^+$, involving the independent migration of the two ions, and flux of $H_3PO_4$, the temperature-dependence profile observed in Figure 3 strongly supports the suggestion that, in the coupled phase, protons traversed

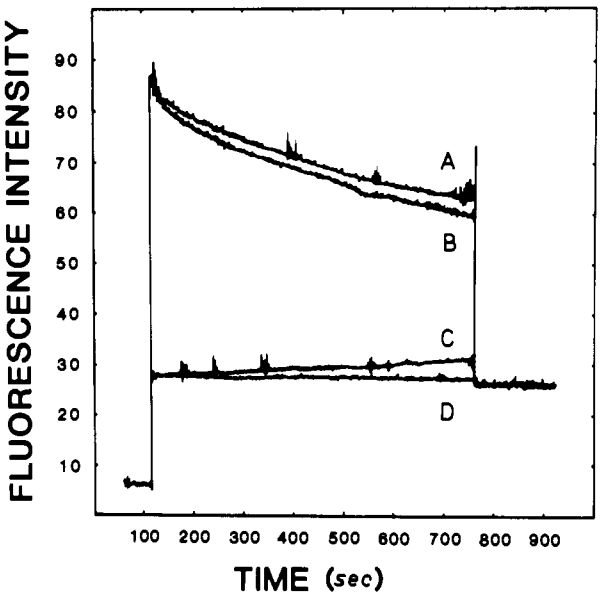


FIGURE 4: Effects of varying phosphate:$H^+$ ratios. DPPC vesicles were diluted into sodium phosphate buffer containing $5 \times 10^{-7}$ M dansylglycine; after mixing, the internal and external buffer compositions were as follows: (A) internal 100 mM sodium phosphate, pH 8.0, external 7 mM sodium phosphate/93 mM sodium sulfate, pH 6.0; (B) internal 100 mM sodium phosphate, pH 8.0, external 100 mM sodium phosphate/26 mM sodium sulfate, pH 6.0; (C) internal 50 mM sodium phosphate, pH 6.0, external 1 mM sodium phosphate/35 mM sodium sulfate, pH 6.0; (D) both internal and external 50 mM sodium phosphate, pH 6.0. In each case, the final lipid concentration was approximately 1 mg/mL, and the sample temperature was 42 °C. Fluorescence measurements were made as described for Figure 2.

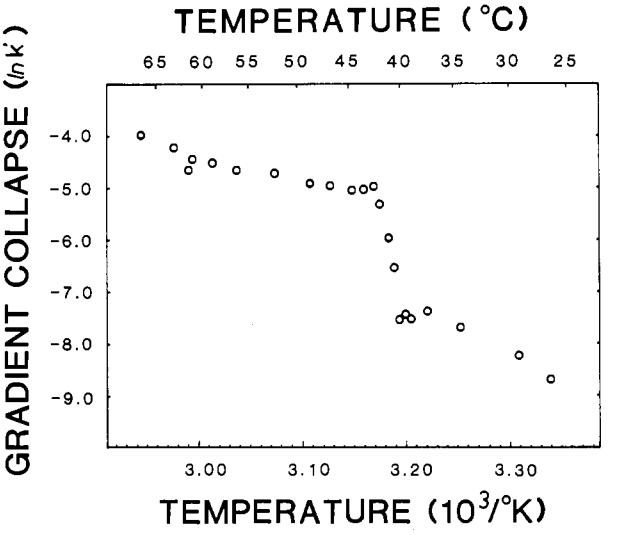


FIGURE 5: Temperature dependence of uncoupled proton flux across DPPC bilayers. Under experimental conditions exactly as described for Figure 3, the initial rate of fluorescence decrease ($k'$) was monitored over a range of temperatures. $k'$ was calculated from a first-order rate equation by inserting, as a terminal value, the fluorescence intensity obtained by extrapolation of the slow phase decline back to the time ΔpH was imposed (when vesicles were diluted into acid medium). $k'$ is plotted here in the form of an Arrhenius function.

the bilayer as components of an electrically neutral complex (phosphoric acid) and that, as a consequence, acid translocation represents an important mechanism for collapse of ΔpH in small vesicular membrane systems.

*Temperature Dependence of Uncoupled Proton Flux.* In marked contrast to the temperature dependence of the coupled phase of proton flux, characterized by a single change in slope at $T_c$, Figure 5 shows that the proton flux which I have

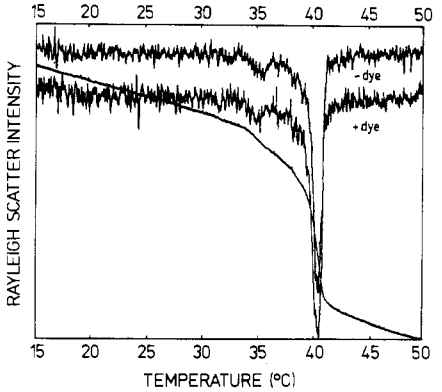


FIGURE 6: Gel–liquid-crystalline phase transition of DPPC bilayers is unaffected by the presence of dansylglycine. Rayleigh light-scattering intensity was recorded continuously as the sample temperature was raised from 15 to 50 °C; both the excitation and emission monochromators were set to 400 nm. The sample consisted of 1.66 mM DPPC in the form of small unilamellar vesicles suspended in 50 mM sodium phosphate, pH 8.0. The scan labeled "–dye" is the first derivative of the Rayleigh scatter profile; the scan labeled "+dye" was obtained after the original sample had been mixed with dansylglycine ($5 \times 10^{-7}$ M final concentration) at 45 °C and then cooled to 15 °C and scanned as the temperature was raised to 50 °C with continuous stirring. The two first-derivative scans have been displaced from each other on the ordinate scale in order to show fine details; they are essentially superimposable.

identified as being uncoupled (the initial flux monitored under conditions of weak buffer capacity) underwent an abrupt change in rate at $T_c$, with no significant difference in slope above and below $T_c$. The very sharp (>12-fold) decrease in rate which occurred at $T_c$ was complete within 2 °C. Although the DPPC vesicles used for this study showed changes in Rayleigh scatter intensity occurring over the temperature range 36–42 °C, the first derivative of the scatter temperature spectrum shows that they underwent $L_\alpha$–$L_\beta$ phase transition at 40–41 °C with a first-derivative half-width of approximately 1.5 °C (Figure 6) and that this transition was unaffected by the presence of dansylglycine. The dramatic discontinuity seen in Figure 5 thus coincided almost exactly, both in location and in duration, with this first-order $L_\alpha$–$L_\beta$ phase transition of the bilayer. Gel permeation chromatography showed that the vesicles used for this study were monodisperse small structures with an average capture volume of 0.5 L/mol of phospholipid (using either $^{22}Na$ or $^{51}Cr$ as the internal marker) with an average vesicle diameter of 35 nm (Lichtenberg et al., 1981). Although the vesicles were small, they were not "limit sized" (Huang, 1969) and thus presumably escaped from some of the phospholipid packing constraints that would otherwise reduce the cooperativity of the main phase transition.

This pattern of temperature dependence clearly shows no similarity to the behavior either of discharged acids (and a variety of other electrically neutral solutes) or of monovalent cations such as sodium or rubidium (El-Mashak & Tsong, 1985); there is, however, a striking resemblance to the known temperature dependence of water permeation rates across similar membranes (Lawaczeck, 1979; Pitterich & Lawaczeck, 1985). This close similarity shown by proton permeation to the behavior of water, revealed also by the observations of Elamrani and Blume (1983), lends strong support for the suggestion that proton permeation is intimately connected to the existence of water within the hydrophobic domain of the membrane.

Water permeates quite readily across most lipid bilayers; it is assumed that the principal barrier to free permeation is the energy cost associated with direct contact between water molecules and the hydrophobic domain created by phospholipid acyl chains within the bilayer. Although the mechanism of water permeation is still poorly understood, it has been suggested that the process involves either diffusion of individual water molecules across the plane of the barrier (Finkelstein & Cass, 1968) or, alternatively, the transient formation of water-filled cavities or channels created by short-lived defects in the membrane structure [Carruthers & Melchior, 1983; for a review, see Deamer & Bramhall (1986)].

The marked similarity existing between rate profiles for water and uncoupled proton permeation immediately suggests a corresponding similarity in the mechanism of permeation for the two species involved. The solubility–diffusion model would presumably seek to explain proton (or $H_3O^+$) permeation in terms of a random dissolution of individual cations into the membrane, followed by passive diffusion across the barrier to the distal side. We are then presented, however, with the difficulty of explaining why $H^+/H_3O^+$ should permeate several orders of magnitude more rapidly, and with such a dramatically different temperature-dependence profile, than $Na^+$, another small cation. Conversely, the transient pore hypothesis would predict that protons move across the membrane barrier when bilayer defects permit the formation of short-lived strands or projections of water into the membrane. This permeation route is apparently not available to sodium ions, implying that the strands do not assume the properties of a column of bulk phase water (which would otherwise be able to accommodate random diffusion of sodium ions). It is worth noting that a strand consisting of a single chain of water molecules ordered by hydrogen bonding would have the selective ability to transfer $H^+$, but no other cation, by Grotthuss conductance (Glasston & Lewis, 1960) provided the mean time for productive chain rearrangement (involving the breaking and re-forming of several intrachain H bonds) was shorter than the mean strand lifetime. The current study provides no direct basis for distinguishing between these various possibilities, but there is a clear implication that, regardless of the precise mechanism, if there is found to be a consistent, strong correlation between water and proton permeability for any given class of membrane (with membranes showing low permeability to protons also showing correspondingly low permeability to water) then measurements of *uncoupled* proton permeation may provide a useful parameter for study of the structure and dynamics of intramembrane water.

**Registry No.** DPPC, 2644-64-6; $H^+$, 12408-02-5; $PO_4^{3-}$, 14265-44-2.

## REFERENCES

Bangham, A. D., de Gier, J., & Greville, G. D. (1967) *Chem. Phys. Lipids 1*, 225–237.
Bramhall, J. (1984) *Biochim. Biophys. Acta 778*, 393–399.
Bramhall, J. (1985) *AOCS Monogr. 13*, 43–50.
Bramhall, J. (1986a) *Biochemistry 25*, 3958–3962.
Bramhall, J. (1986b) *Biochemistry 25*, 3479–3486.
Cafiso, D. S., & Hubbell, W. L. (1983) *Biophys. J. 44*, 49–57.
Carruthers, A., & Melchior, D. L. (1983) *Biochemistry 22*, 5797–5807.
Cornell, B. A., & Separovic, F. (1983) *Biochim. Biophys. Acta 733*, 189–193.
Deamer, D. W., & Nichols, J. W. (1983) *Proc. Natl. Acad. Sci. U.S.A. 80*, 165–168.
Deamer, D. W., & Bramhall, J. S. (1986) *Chem. Phys. Lipids 40*, 167–188.
Elamrani, K., & Blume, A. (1983) *Biochim. Biophys. Acta 727*, 22–30.
El-Mashak, E. M., & Tsong, T. Y. (1985) *Biochemistry 24*, 2884–2888.

Engelbert, H.-P., & Lawaczeck, R. (1985) *Ber. Bunsen-Ges. Phys. Chem. 89*, 754–759.
Finkelstein, A., & Cass, A. (1968) *J. Gen. Physiol. 52*, 145s–172s.
Forgac, M., Cantley, L., Wiedenmann, B., Altsteil, L., & Branton, D. (1983) *Proc. Natl. Acad. Sci. U.S.A. 80*, 1300–1303.
Garcia, M. L., Kitada, M., Eisenstein, H. C., & Krulwich, T. A. (1984) *Biochim. Biophys. Acta 766*, 109–115.
Glasston, S., & Lewis, D. (1960) *Elements of Physical Chemistry*, p 446, Van Nostrand, New York.
Gutknecht, J., & Walter, A. (1981) *Biochim. Biophys. Acta 641*, 183–188.
Helenius, A., Kielian, M., Wellsteed, J., Mellman, I., & Rudnick, G. (1985) *J. Biol. Chem. 260*, 5691–5697.
Hinkle, P. C., & McCarty, R. E. (1978) *Sci. Am. 238*, 104–123.
Huang, C. (1969) *Biochemistry 8*, 344–352.
Jähnig, F., & Bramhall, J. (1982) *Biochim. Biophys. Acta 690*, 310–313.
Krishnamoorthy, G., & Hinkle, P. C. (1984) *Biochemistry 23*, 1640–1645.
Lawaczeck, R. (1979) *J. Membr. Biol. 51*, 229–261.
Lichtenberg, D.; Freire, E., Schmidt, C. F., Barenholz, Y., Felgner, P. L., & Thompson, T. E. (1981) *Biochemistry 20*, 3462–3467.
Lis, L., McAllister, M., Fuller, N., Rand, R. P., & Parsegian, V. A. (1982) *Biophys. J. 37*, 657–666.
London, E., & Feigenson, G. W. (1978) *Anal. Biochem. 88*, 203–211.
Mitchell, P. (1979) *Science (Washington, D.C.) 206*, 1148–1159.
Mitchell, P., & Moyle, J. (1968) *Eur. J. Biochem. 4*, 530–539.
Nichols, J. W., & Deamer, D. W. (1980) *Proc. Natl. Acad. Sci. U.S.A. 77*, 2038–2042.
Nozaki, Y., & Tanford, C. (1981) *Proc. Natl. Acad. Sci. U.S.A. 78*, 4324–4328.
Papahadjopoulos, D., Jacobson, K., Nir, S., & Isac, T. (1973) *Biochim. Biophys. Acta 311*, 330–348.
Parsegian, A. (1969) *Nature (London) 221*, 844–846.
Pitterich, H., & Lawaczeck, R. (1985) *Biochim. Biophys. Acta 821*, 233–242.
Small, D. M. (1967) *J. Lipid Res. 8*, 551–557.

# Mechanism of Action of Inter-$\alpha$-trypsin Inhibitor†

Charlotte W. Pratt and Salvatore V. Pizzo*
*Departments of Biochemistry and Pathology, Duke University Medical Center, Durham, North Carolina 27710*
*Received August 27, 1986; Revised Manuscript Received December 11, 1986*

ABSTRACT: Inter-$\alpha$-trypsin inhibitor (I$\alpha$I) is a unique proteinase inhibitor that can be proteolyzed by the same enzymes that are inhibited, to generate smaller inhibitors. This study examines the reactions of I$\alpha$I with trypsin, chymotrypsin, plasmin, and leukocyte elastase. Complexes of I$\alpha$I and proteinase were demonstrated by gel filtration chromatography. Complete digestion of I$\alpha$I by each proteinase was not accompanied by a comparable loss of inhibition of that enzyme or a different enzyme. Following proteolysis, inhibitory activity was identified in I$\alpha$I fragments of molecular weight 50 000–100 000 and less than 40 000. Addition of a second proteinase inhibitor prevented proteolysis. Both I$\alpha$I and its complex with proteinase were susceptible to degradation. Kinetic parameters for both the inhibition and proteolysis reactions of I$\alpha$I with four proteinases were measured under physiological conditions. On the basis of these results, a model for the mechanism of action of I$\alpha$I is proposed: Proteinase can react with either of two independent sites on I$\alpha$I to form an inhibitory complex or a complex that leads to proteolysis. Both reactions occur simultaneously, but the inhibitory capacity of I$\alpha$I is not significantly affected by proteolysis since the product of proteolysis is also an inhibitor. For a given proteinase, the inhibition equilibrium constant and the Michaelis constant for proteolysis describe the relative stability of the inhibition and proteolysis complexes; the second-order rate constants for inhibition and proteolysis indicate the likelihood of either reaction. The incidence of inhibition or proteolysis reactions involving I$\alpha$I in vivo cannot be assessed without knowledge of the exact concentrations of inhibitor and proteinases; however, analysis of inhibition rate constants suggests that I$\alpha$I might be involved in plasmin inhibition.

Plasma proteinase inhibitors are implicated in the regulation of proteolytic processes such as coagulation, fibrinolysis, and inflammation. Among the best-studied inhibitors are the serine proteinase inhibitors of the $\alpha_1$-proteinase inhibitor class which share a common mechanism of action [for a review, see Travis and Salvesen (1983)]. The classification of a number of other proteinase inhibitors is incomplete owing to insufficient knowledge of their inhibitory mechanisms. One such protein is inter-$\alpha$-trypsin inhibitor (I$\alpha$I).[1]

I$\alpha$I consists of a single glycopeptide chain of molecular weight 160 000–200 000 (Steinbuch, 1976), and it appears in

† This work was supported by National Heart, Lung, and Blood Institute Grant HL-24066.

[1] Abbreviations: I$\alpha$I, inter-$\alpha$-trypsin inhibitor; I′, proteolyzed form of inter-$\alpha$-trypsin inhibitor; HEPES, *N*-(2-hydroxyethyl)piperazine-*N*′-2-ethanesulfonic acid; Bz, benzoyl; Boc, *tert*-butoxycarbonyl; pNA, *p*-nitroanilide; 7AMC, 7-(aminomethyl)coumarin; $NaDodSO_4$, sodium dodecyl sulfate.

0006-2960/87/0426-2855$01.50/0 